



# MendelNet

Conference Brno 2019



Editors:

Radim Cerkal

Natálie Březinová Belcredi

Lenka Prokešová

Aneta Pilátová

Proceedings of 26<sup>th</sup>  
International PhD Students Conference

6-7 November 2019, Brno, Czech Republic

**Mendel University in Brno**  
**Faculty of AgriSciences**



**MendelNet 2019**

Proceedings of 26<sup>th</sup> International PhD Students Conference  
6–7 November 2019, Brno, Czech Republic

Editors: Radim Cerkal, Natálie Březinová Belcredi, Lenka Prokešová, Aneta Pilátová

## Sensitive biosensor for detection oncogenic miRNA-21

Veronika Vanova<sup>1</sup>, Eliska Sedlackova<sup>1,2</sup>, David Hynek<sup>1,2</sup>, Lukas Richtera<sup>1,2</sup>,  
Vojtech Adam<sup>1,2</sup>

<sup>1</sup>Department of Chemistry and Biochemistry  
Mendel University in Brno  
Zemedelska 1, 613 00 Brno

<sup>2</sup>Central European Institute of Technology,  
Brno University of Technology,  
Purkynova 123, 612 00 Brno  
CZECH REPUBLIC

veronika.vanova@mendelu.cz

**Abstract:** The aim of this study was to prepare a sensitive electrochemical biosensor for detection of oncogenic miRNA-21 as a potential biomarker for early detection of cancer. MicroRNAs (miRNAs) are small noncoding RNA, which play an important role in the regulation of gene expression. miRNAs are present in extracellular fluids like urine, serum, etc. in extremely low concentration. It is important for the biosensor to detect extremely low concentrations of specific miRNA as potential biomarkers. The aim of this experiment was designing, preparing and optimizing a sensitive and selective biosensor for the detection of miRNA-21. A biosensor was prepared to detect the lowest concentration of miRNA-21 in the sample. The linear concentration range for the calibration curve was 1 fM to 10 nM. LOD was 1 fM and obtained from the regression equation was 3.2 zM and LOQ was 10.8 zM. Subsequently, prepared biosensor was measured in artificial urine (AU) samples to verify the functioning of the sensor in induced real conditions. The results showed a minimal effect of the matrix for the determination of the target miRNA.

**Key Words:** nucleic acids, miRNA, electrochemical detection, biosensor

### INTRODUCTION

In the field of science, the possibility of biomarker detection as an indicator of biological or pathological state of the organism could be a way to simplify, accelerate and refine the diagnosis of diseases. A particular possibility of such biomarkers is a miRNA molecule. It has been found that miRNA has an irreplaceable role in influencing the expression of large number of genes and also that the level of these molecules can be observed in various extracellular fluids such as e.g. urine or plasma (Krol et al. 2010).

Another interesting finding with these molecules is that the expression of some particular miRNAs varies considerably in oncological diseases (Rupaimoole and Slack 2017). Therefore, the level of these miRNAs varies significantly (increases / decreases), which can be detected non-invasively in these extracellular fluids. This knowledge has led scientists to wonder how these molecules could be detected in clinical practice as easily, as accurately, as quickly and as cheaply as possible (Cho 2010). Currently, the most commonly used methods are Northern blotting or RT-PCR (de Planell-Saguer and Rodicio 2013) but these methods are often laborious and costly. Therefore, new approaches are being sought to detect them in a simple, cost effective manner with higher selectivity and enhanced sensitivity (Tian et al. 2015). One such detection approach is to create a sensitive electrochemical biosensor for miRNA detection. An example of such biosensor is blood glucose meter which is already in practice for diabetes detection with high sensitivity and specificity. The advantage of such sensors is that they can detect the level of the substance in the body very quickly. A very small sample is sufficient and should be affordable when put into practice (Kilic et al. 2018, Hamidi-Asl et al. 2013).

## MATERIALS AND METHODS

### Chemicals and apparatuses

We used 1.0  $\mu\text{m}$ , 0.3  $\mu\text{m}$  and 0.05  $\mu\text{m}$  Alumina Slurry suspension and 0.5  $\mu\text{m}$  Diamond suspension (Electron Microscopy Sciences, Hatfield, United Kingdom) for electrode polishing, Ethanol absolute (VWR chemicals, Randor, Pennsylvania, USA), Acetone (VWR chemicals, Randor, Pennsylvania, USA), MiliQ water (18.20 M $\Omega$ /cm).

Phosphate buffered saline (PBS) (pH 7, 25 mM) was prepared by mixing 20.0 g sodium chloride (NaCl), 0.5 g Potassium chloride (KCl), 3.6 g Sodium phosphate dibasic (Na<sub>2</sub>HPO<sub>4</sub>) and 0.6 g Potassium dihydrogen phosphate (KH<sub>2</sub>PO<sub>4</sub>) (Sigma-Aldrich, St. Louis, MO, USA) into 1000 ml of MiliQ water. 10 mM 1-amino-2-naphthol-4-sulfonic acid (AN-SO<sub>3</sub><sup>-</sup>) (Sigma-Aldrich, St. Louis, MO, USA) was diluted in PBS.

Other chemicals which we used: 40 mM, 16.7 mg Phosphorus pentachloride (PCl<sub>5</sub>) in acetone (2 ml), Tris-EDTA (TE buffer) pH 8 (Sigma-Aldrich, St. Louis, MO, USA).

All measurements were taken in 5 mM Potassium hexacyanoferrate (II) trihydrate K<sub>4</sub>[Fe(CN)<sub>6</sub>]/5 mM Potassium hexacyanoferrate(III) K<sub>3</sub>[Fe(CN)<sub>6</sub>] in 0.1 M KCl (Sigma-Aldrich, St. Louis, MO, USA).

Oligonucleotides were purchased also from Sigma-Aldrich:

DNA probe (anti-miRNA-21): 5'-NH<sub>2</sub>-C<sub>6</sub>-TCAACATCAGTCTGATAAGCTA-3'

miRNA-21: 5'-UAGCUUAUCAGACUGAUGUUGA-3'.

Artificial urine was prepared into 250 ml MiliQ water by stirring 1.90 g KCl, 4.25 g NaCl, 12.25 g urea, 0.59 g Potassium dihydrogen phosphate (KH<sub>2</sub>PO<sub>4</sub>), 0.52 g Magnesium sulfate heptahydrate (MgSO<sub>4</sub> · 7H<sub>2</sub>O), 0.52 g Citric acid, 0.17 g Ascorbic acid, 0.70 g Creatinine, 0.32 g Sodium hydroxide (NaOH), 0.24 g Sodium bicarbonate (NaHCO<sub>3</sub>), 0.14 ml Sulfuric acid (99%, H<sub>2</sub>SO<sub>4</sub>). Solution was diluted by MiliQ water into 500 ml.

### Preparation and modification of electrode

First of all, the glassy carbon electrode (GCE) was polished by using 1.0; 0.3; 0.05  $\mu\text{m}$  Alumina slurry and 0.5  $\mu\text{m}$  Diamond suspension each for 90 s. Between each step, electrodes were sonicated in acetone, ethanol, and water for 90 s respectively. And finally, GCE was dried under the argon gas.

The second step of modification was electrodeposition of 1-amino-2-naphthol-4-sulfonic acid (AN-SO<sub>3</sub><sup>-</sup>) (10 mM) in PBS buffer (25 mM, pH 7.0). It was done by cyclic voltammetry (CV) scanning between +1.5 V and -0.5 V with the scan rate 20 mVs<sup>-1</sup> and 8 cycles. CV was performed by using a three-electrode system containing Ag/AgCl as a reference electrode, platinum wire as a counter electrode and GCE as a working electrode. In this step was obtained. AN-SO<sub>3</sub><sup>-</sup> modified GCE (Wang et al. 2013).

Subsequently the electrode was immersed in a solution of PCl<sub>5</sub> (40 mM) in acetone (absolute) for 30 min to transfer the sulfonic groups on the sulfonyl groups on the GCE modified with AN-SO<sub>3</sub><sup>-</sup> (Chen et al. 2008).

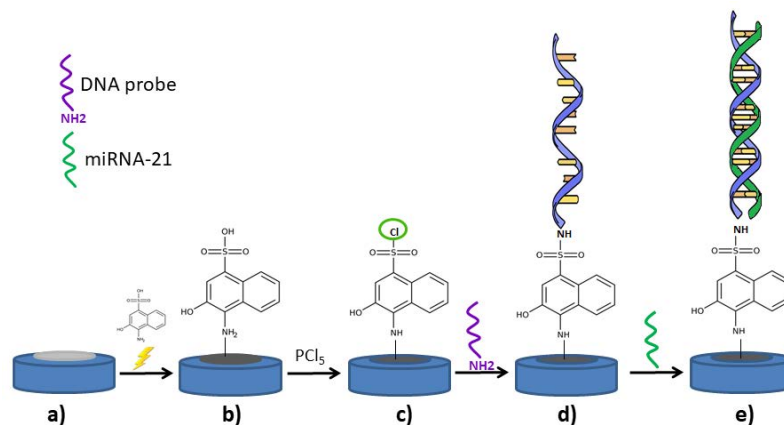
DNA oligonucleotides with a sequence complementary to target miRNA were defrosted and diluted in TE buffer to 1  $\mu\text{M}$  concentration and subsequently heated up to 80 °C for 2 min. Then they were dropped on the surface of GCE in 10  $\mu\text{l}$  volume (Smith et al. 2017). Oven was heated to 80 °C and the modified electrodes with oligonucleotides were placed inside for 90 min. After drying, electrode was slightly rinsed in TE buffer and then measured with CV and EIS. The hybridization was done at room temperature for 45 min by incubation in the exact concentration of target miRNA diluted in TE buffer and artificial urine (Figure 1).

### Electrochemical measurement

Electrochemical measurements were taken in every step of modification, before and after the hybridization. We were using cyclic voltammetry (CV) method and electrical impedance spectroscopy method (EIS).

CV was running at a potential between +0.7 V and –0.3 V with scan rate 20 mVs<sup>-1</sup> and 8 cycles. EIS was set at a DC potential of 0.23 V between frequencies of 0.01 Hz to 10 kHz with an AC of 5 mV (Wang et al. 2013).

Figure 1 a) bare GCE electrode b) electrodeposition of AN–SO<sub>3</sub><sup>-</sup> on GCE c) sulfonation d) DNA probe immobilization e) hybridization target miRNA-21



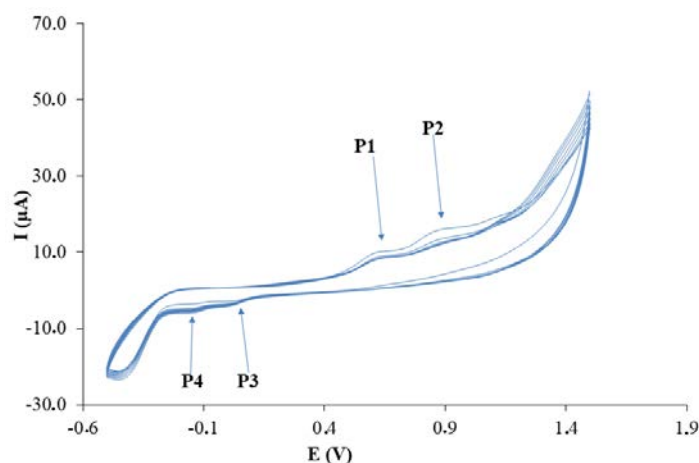
## RESULTS AND DISCUSSION

### Modification of the electrode

#### Electrodeposition of AN–SO<sub>3</sub><sup>-</sup> on GCE

In this part of the modification, we modified GCE by electrochemical immobilization of the AN–SO<sub>3</sub><sup>-</sup> (Nomura 1982) on the electrode surface. Deposition layer of the AN–SO<sub>3</sub><sup>-</sup> were increased with the continuous growth of the CV cycles. As Figure 2 observe there are two reduction peaks at position –0.013 V (P3), –0.200 V (P4) and two oxidation peaks +0.600 V (P1) and +0.900 V (P2). This record shows us that the electrochemical deposition of AN–SO<sub>3</sub><sup>-</sup> on the GCE surface is irreversible and with increasing cycles the peaks gradually decrease, which proves the continuous growth of the AN–SO<sub>3</sub><sup>-</sup> film. Successful electrodeposition was also displayed in the change of electrode colour from shiny silver to matt grey.

Figure 2 Electrodeposition of AN–SO<sub>3</sub><sup>-</sup> on GCE



#### Step-by-step modification process of the electrode

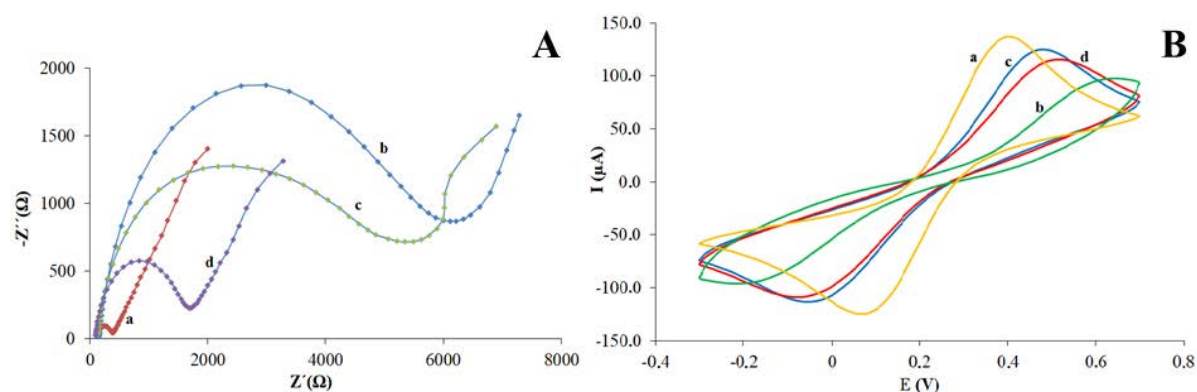
CV and EIS methods were done in each step of the electrode modification. Every step was measured in 5 mM (K<sub>4</sub>[Fe(CN)<sub>6</sub>])/ 5 mM K<sub>3</sub>[Fe(CN)<sub>6</sub>] in 0.1 M KCl electrolyte.

Cyclic voltammetry: by measuring the bare electrode we occurred pair of significant oxidation-reduction peaks (Figure 3B a). However, after the electrodeposition of AN–SO<sub>3</sub><sup>-</sup> on GCE

the peaks decreased dramatically in comparison with those of on bare GCE. AN-SO<sub>3</sub><sup>-</sup> layer partially prevents electron transfer of electrolyte ions to the electrode surface as a result of electrostatic repulsion force (Figure 3B b). After incubation in a solution of PCl<sub>5</sub>, the redox peaks increased (Figure 3B c). Further, after application and incubation of the DNA probe on the modified electrode, the redox peaks decreased again (Figure 3B d). This is the affirmation that the immobilization of the probe was successful (Wang et al. 2013).

With EIS, we can monitor the changes of the diameter in Nyquist plots in different steps of the modification. The diameter of the semicircle reflect the resistance of electron transfer on the electrode surface. The lowest resistance was observed at bare GCE (Figure 3A a). The AN-SO<sub>3</sub><sup>-</sup> electrodeposition leads to a significantly higher resistance (Figure 3A b). After reacting with PCl<sub>5</sub>, the resistance is again markedly increased (Figure 3A c). Finally, the resistance of the immobilized probe was decreased again (Figure 3A d) (Smith et al. 2017, Wang et al. 2013).

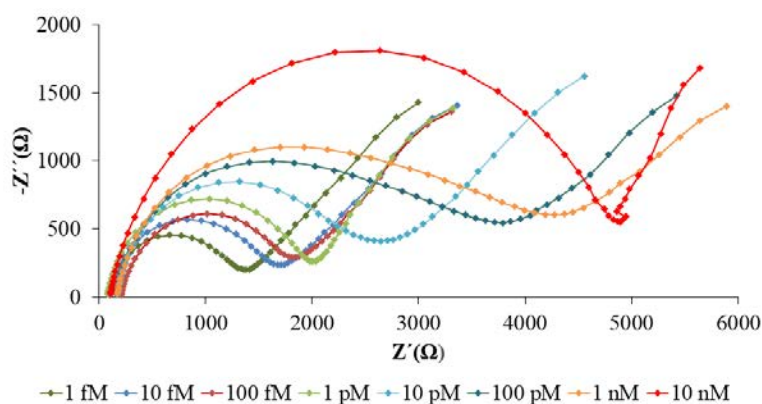
Figure 3 A) Nyquist plots, B) CV voltammograms showing: a) unmodified electrode b) electro-deposition AN-SO<sub>3</sub><sup>-</sup> c) modification with PCl<sub>5</sub> d) probe immobilization



#### miRNA hybridization with DNA probe in different concentrations

In this part of the experiment, the sensitivity of the designed biosensor was tested. For this part of the study we were using only EIS method for its better sensitivity. The aim of this study was to prepare as sensitive biosensor as possible. We measured different concentrations of miRNA-21 ranging from 10<sup>-8</sup> M (10 nM) to 10<sup>-15</sup> M (1 fM) dissolved in TE buffer (Figure 4). Irregular results were obtained at lower concentrations than 1 fM, therefore they were not included in the calibration curves. The values that were used in the calibration curve were calculated using NOVA 1.8 software as the value of the difference between the final point and the start point of the Nyquist semi-circle graph.

Figure 4 Nyquist plots from measurement of different concentrations of miRNA-21 in TE buffers by EIS method



#### Calibration curves

Calibration curves were generated according to data measured by EIS. Concentration values are reported in the calibration curves as log *c* (M) values to show their linear dependence. For better

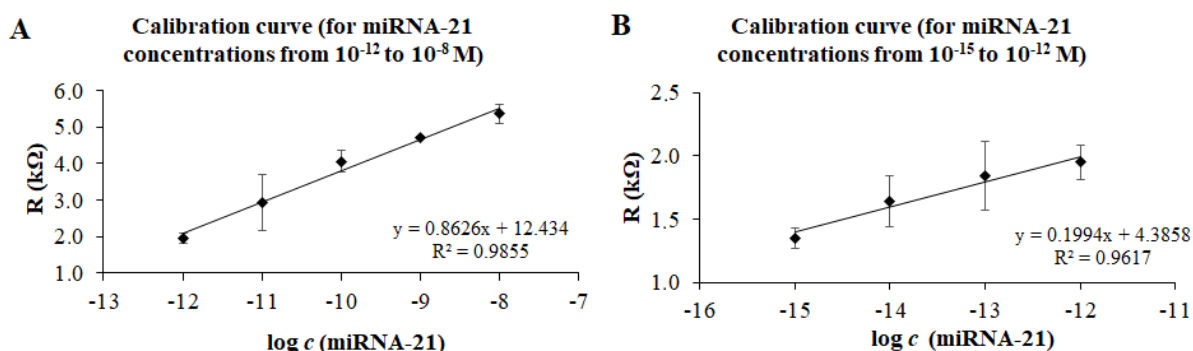
accuracy of the regression coefficient ( $R^2$ ), the calibration data were divided into two calibration curves. The part with concentration values from 10 nM to 1 pM reached an accuracy of  $R^2 = 0.9885$  and the part with concentration values from 1 pM to 1 fM concentration had  $R^2 = 0.9617$  (Figure 5).

LOD and LOQ values were counting true the regression equation. LOD 3.2 zM and LOQ 10.8 zM (Table 1). However, these values were very low. Practically, we were able to measure the lowest 1 fM concentration, which is still low enough for measuring miRNA in real samples. According to Smith et al. (2017) the concentrations of miRNA-21 which were measured in real samples of urine were around  $10^{-9} - 10^{-11}$  M. These values are fitting enough into the calibration range.

Table 1 Analytical table for LOD and LOQ calculation.

Sample	Regression Equation	Linear dynamic range $\log c$ (M)	$R^2$	LOD (zM)	LOQ (zM)	RSD (%)
miRNA-21	$y = 0.8626x + 12.434$	-8 to -12	0.9855	3.2	10.8	2.5
	$y = 0.1994x + 4.3858$	-12 to -15	0.9617			

Figure 5 Calibration curves: A) concentration values from  $10^{-8}$  to  $1^{-12}$  M B) concentration values from  $1^{-12}$  to  $1^{-15}$  M.



### Measurement in artificial urine

In the last section, we measured miRNA-21 oligonucleotides dissolved in AU. Concentration levels which have been measured in AU samples have been selected according to the values corresponding to concentrations in real urine samples. The chosen values were  $10^{-11}$ ,  $10^{-10}$ ,  $10^{-9}$  M. To check the measurements, the measured data from AU were fitted into the regression equation from the calibration curve A (Figure 5A) and calculated. We compared the measured data of AU and the calculated data in percentage. After the evaluating added concentrations and the calculated concentrations (recovery) (Tab.2), we achieved sufficient measurement accuracy, which suggests that the measurement was performed correctly and the artificial urine matrix does not affect the correct functionality and sensitivity of the prepared biosensor.

Table 2 Values of real concentrations of miRNA-21 in AU compared to the values calculated from the regression equation and their percentage expression

Concentration (added)		Calculated concentration	Recovery (%)
$\log c$ (M)	(M)	$\log c$ (M)	% $\log c$ (M)
-11	$1 \times 10^{-11}$	-11.32	103
-10	$1 \times 10^{-10}$	-9.86	99
-9	$1 \times 10^{-9}$	-9.81	109

### CONCLUSION

To sum up we have designed, prepared and tested a stable concept of a biosensor for detection of oncogenic miRNA-21. We also demonstrated the functionality of this biosensor to determine miRNA samples in an artificial urine matrix. For practical use in the future, it will be necessary to test the biosensor in real urine samples at clinical patients.

## ACKNOWLEDGEMENTS

This research was carried out under the project CEITEC 2020 (LQ1601) with financial support from the Ministry of Education, Youth and Sports of the Czech Republic under the National Sustainability Programme II.

The research was financially supported by IGA MENDELU AF-IGA2019-IP059.

## REFERENCES

- Chen, J.H. et al. 2008. Electrochemical Biosensor for Detection of BCR/ABL Fusion Gene Using Locked Nucleic Acids on 4-Aminobenzenesulfonic Acid-Modified Glassy Carbon Electrode. *Analytical Chemistry*, 80(21): 8028–8034.
- Cho, W.C.S. 2010. MicroRNAs: Potential biomarkers for cancer diagnosis, prognosis and targets for therapy. *International Journal of Biochemistry & Cell Biology*, 42(8): 1273–1281.
- de Planell-Saguer, M., Rodicio, M.C. 2013. Detection methods for microRNAs in clinic practice. *Clinical Biochemistry*, 46(10–11): 869–878.
- Hamidi-Asl, E. et al. 2013. A review on the electrochemical biosensors for determination of micro RNAs. *Talanta*, 115: 74–83.
- Kilic, T.A. et al. 2018. MicroRNA biosensors: Opportunities and challenges among conventional and commercially available techniques. *Biosensors & Bioelectronics*, 99: 525–546.
- Krol, J. et al. 2010. The widespread regulation of microRNA biogenesis, function and decay. *Nature Reviews Genetics*, 11(9): 597–610.
- Nomura, T. 1982. Alternating-Current Polarographic-Determination of Microgram Amounts of Iodide-Ion by Means of the Catalytic-Oxidation of 1-Amino-2-Naphthol-4-Sulfonic Acid. *Journal of Electroanalytical Chemistry*, 139(1): 97–104.
- Rupaimoole, R., Slack F.J. 2017. MicroRNA therapeutics: towards a new era for the management of cancer and other diseases. *Nature Reviews Drug Discovery*, 16(3): 203–221.
- Smith, D.A. et al. 2017. Electrochemical detection of urinary microRNAs via sulfonamide-bound antisense hybridisation. *Sensors and Actuators B-Chemical*, 253: 335–341.
- Tian, T. et al. 2015. A review: microRNA detection methods. *Organic & Biomolecular Chemistry* 13(8): 2226–2238.
- Wang, Q.X. et al. 2013. A sensitive DNA biosensor based on a facile sulfamide coupling reaction for capture probe immobilization. *Analytica Chimica Acta*, 788: 158–164.

<b>Name of publication:</b>	MendelNet 2019 <i>Proceedings of 26<sup>th</sup> International PhD Students Conference</i>
<b>Editors:</b>	Assoc. Prof. Ing. Radim Cerkal, Ph.D. Ing. Natálie Březinová Belcredi, Ph.D. Ing. Lenka Prokešová Mgr. Aneta Pilátová
<b>Publisher:</b>	Mendel University in Brno Zemědělská 1665/1 613 00 Brno Czech Republic
<b>Year of publication:</b>	2019
<b>Number of pages:</b>	709
<b>ISBN:</b>	978-80-7509-688-3

Contributions are published in original version, without any language correction.